Supporting Information

Enhancement of ultra-high rate chargeability by interfacial nanodot $BaTiO_3$ treatment on $LiCoO_2$ cathode thin film batteries

Sou Yasuhara[†,‖], Shintaro Yasui[*,†,‖], Takashi Teranishi[‡,‖], Keisuke Chajima[‡], Yumi Yoshikawa[‡], Yutaka Majima[†], Tomoyasu Taniyama[†,§], and Mitsuru Itoh[*,†]

† Laboratory for Materials and Structures, Tokyo Institute of Technology, Yokohama 226-8503, Japan

‡ Graduate School of Natural Science and Technology, Okayama University, Okayama 700-8530, Japan

§ Department of Physics, Nagoya University, Nagoya 464-8601, Japan

*E-mail address: yasui.s.aa@m.titech.ac.jp

*E-mail address: itoh.m.aa@m.titech.ac.jp

Experimental procedure

Finite element method: The current density mapping near the TPI were calculated by the finite element method using ANSYS, HFSS ver. R17.1. Figure 1a shows a modeled structure of the TPI. We assumed the dielectric constants and losses of BTO and SEI were 300[1] and 10%, and 10 and 10%, respectively. LCO and electrolyte were set to the resistance. Thicknesses of LCO, BTO and SEI were set to 150 nm, 10 nm, and 2 nm, respectively.

Preparation of cathode epitaxial thin films: LCO cathode thin films were prepared on a current corrector of $SrRuO_3$-covered $SrTiO_3(100)$ single crystal substrates by pulsed laser deposition using the fourth harmonic wave (266 nm) of a Nd:YAG laser. The substrate for epitaxial film growth was a $SrTiO_3(100)$ single crystal.[2–4] Li 60% excess ceramic ($Li_{1.6}CoO_2$) target was used for deposition because Li evaporated during deposition under vacuum conditions.[5,6] We prepared two types of BTOs on LCO thin films by adjusting $p(O_2)$ during deposition. One was layer-by-layer growth under $p(O_2)$ of 200 mTorr and the other was island growth under $p(O_2)$ of 2 Torr. Layer-by-layer growth realized the thin film form (Planar BTO), whereas the island BTO was grown with nanodots on LCO (called "Dot BTO"). Planar BTO was almost covered by BTO on the LCO surface. On the other hand, the LCO surface contained some BTO nanodots, but it was not fully covered. As a control experiment, pure LCO thin films without BTO were prepared.

The crystal structures and epitaxial relationships were evaluated by out-of-plane X-ray diffraction (XRD) and XRD reciprocal space mappings measured by Rigaku Smartlab. Plan-view and cross-sectional scanning electron microscope (SEM) images were

obtained using Hitachi S-8000. Cross sectional high-angle annular dark field (HAADF) scanning transmission electron microscope (STEM) and energy dispersive X-ray spectroscopy (EDX) mapping images were measured by JEOL JEM-2100F.

Coin-cell assembly and electrochemical measurement: Coin-type 2032 cells were assembled in an Ar-filled glove box using prepared thin film as the cathode, Li metal as the anode, and $LiPF_6$ (EC : DEC = 3 : 7 v/v) as the electrolyte. These cells were cycled within a voltage window of 3.3–4.2 V *vs.* Li^+/Li range. The charge-discharge measurements were performed using the following parameters: charge, OCV (1 h), discharge, and OCV (1 h). The cells were initially charged and discharged at 1C (1C = 160 mA/g) for five cycles. Then the charge–discharge rate was increased stepwise from 2C, 5C, 10C, 20C, 50C and finally to an ultrahigh rate of 100C. Each stepwise increase was repeated for five cycles. In the AC impedance measurements, the frequency ranged from 50 mHz to 1 MHz, while the applied AC voltage was 50 mV. The AC impedance measurement was performed before charge (after OCV) and after charge (after OCV) at 1C, respectively.

Preparation and characterization of 10C Mask films: The patterned $BaTiO_3$ of 50 nm was deposited on $LiCoO_2/SrRuO_3/SrTiO_3(100)$ epitaxial thin film by using the shadow mask (100 μm□, coverage of 25%) via PLD method. Coin-type 2032 cells were assembled in an Ar-filled glove box using prepared cathode thin films, Li metal as anode, and $LiPF_6$ (EC : DEC = 3 : 7 v/v) as the electrolyte. These cells were cycled within a voltage window of 3.3–4.2 V vs. the Li^+/Li range. The charge-discharge measurements were performed using the following parameters: 1 C for three cycles, 2C for 5 cycles, 5C

for 5 cycles and 10C for 5 cycles. The discharge capacities were shown in Fig. S9. After the electrochemical measurements, the coincell was disassembled and washed with DEC liquid in pure Ar-filled glove box. The obtained sample is called as 10C Mask. The surface profile and SEM images were measured by Kosaka. Lab. Ltd., ET200 and Hitachi, S-4800, respectively. The transcribed BTO pads had about 130 μm square due to a wraparound of BTO in the vicinity of the mask edge during deposition. In addition, the thickness gradient was observed at the edge of BTO pads.

Figure S1 shows a model of the triple-phase interface composed of LCO, electrolyte, and BTO as well as the solid electrolyte interface (SEI). In general, SEIs must be created at the interface between the cathode and liquid electrolyte. Here, a small dielectric constant and dielectric loss of 10 and 10% in SEI are respectively assumed because the SEI may be decomposed materials from $LiPF_6$ and EC/DEC solvent. Additionally, we supposed that the dielectric constants and dielectric loss of BTO are 300 and 10%, respectively. Figure 1b shows the current density mapping results by FEM.

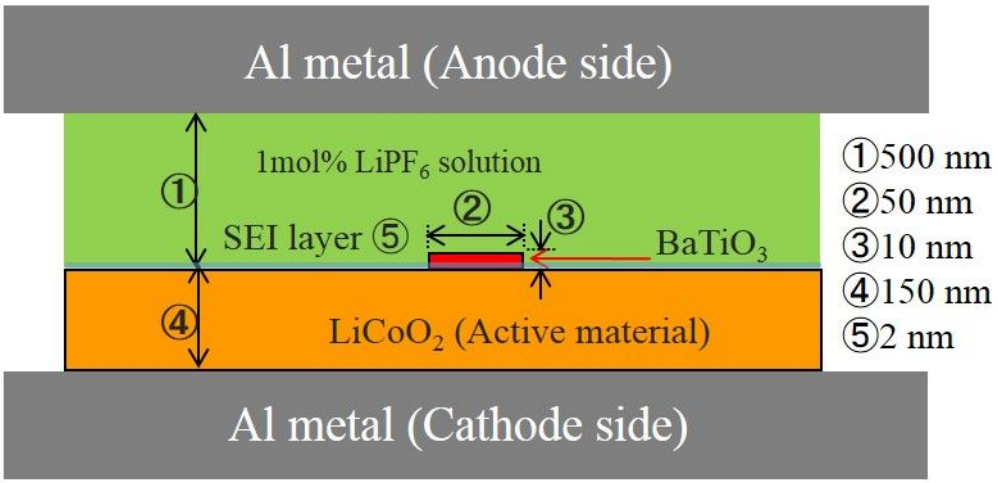

Figure S1. Schematic of the modeled structure for ANSYS HFSS calculations.

Figure S2 shows the out-of-plane XRD results of Bare, Planar BTO, and Dot BTO. Only LCO*104*, SRO$00l_c$ and STO*00l* diffraction peaks appear without impurity peaks. BTO diffraction peaks are not observed by XRD measurements due to the thin BTO layer in both Planar BTO and Dot BTO.

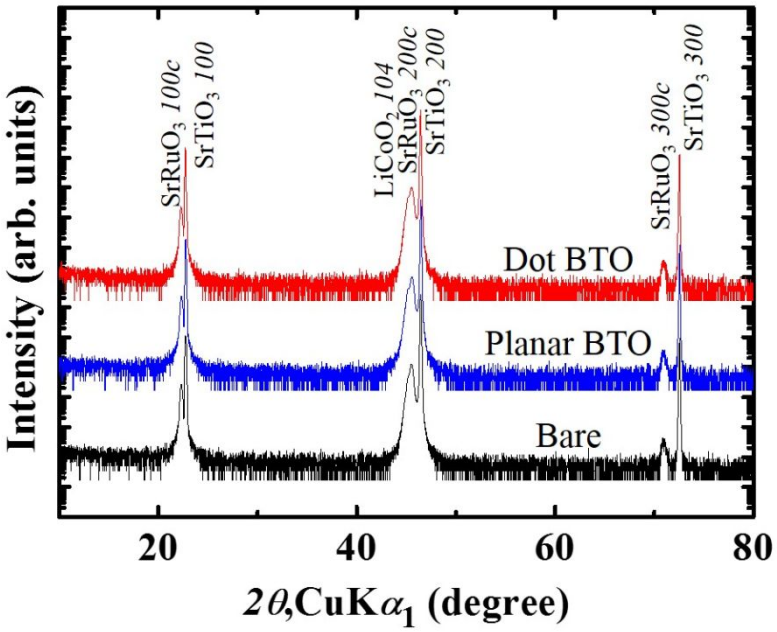

Figure S2. XRD out-of-plane results of Dot BTO (red), Planar BTO (blue), and Bare (black).

Figure S3 shows the reciprocal space mapping of Bare along STO[100] and STO[110] axis. The thin film does not have an impurity phase in the in-plane direction. Figure S4 shows the XRD phi-scan of LCO{*003*} and STO{*111*} diffractions. Similar to the STO substrate, LCO{*003*} has a four-fold symmetry. These results indicate that LCO is epitaxially grown on an SRO/STO100 substrate. The epitaxial relationship is confirmed as follows: LCO(104)//STO(001), LCO(0-14)//STO(100) and LCO(-108)//STO(110).

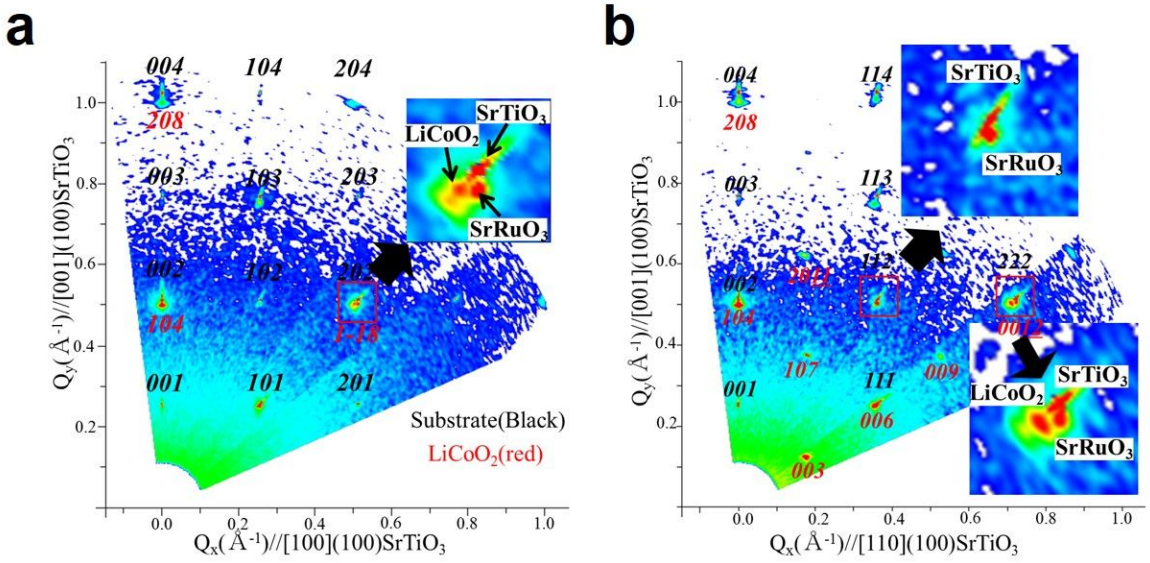

Figure S3. XRD reciprocal space mappings of (a) Bare along [100](100)$SrTiO_3$ (a) and (b) along [110](100)$SrTiO_3$.

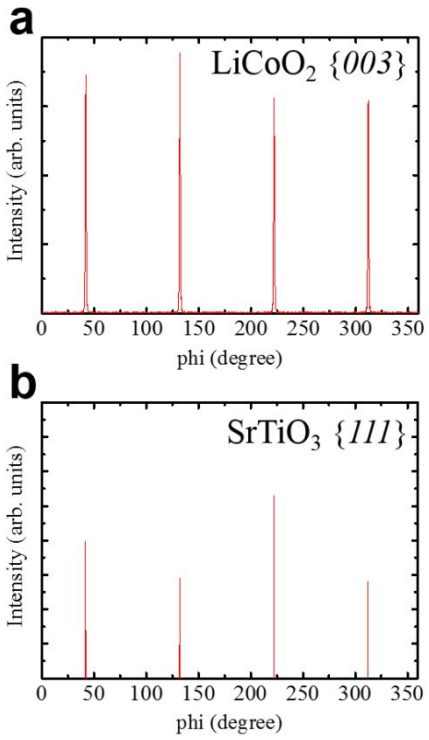

Figure S4. XRD phi-scans of (a) $LiCoO_2${*003*} and (b) $LiCoO_2${*111*}

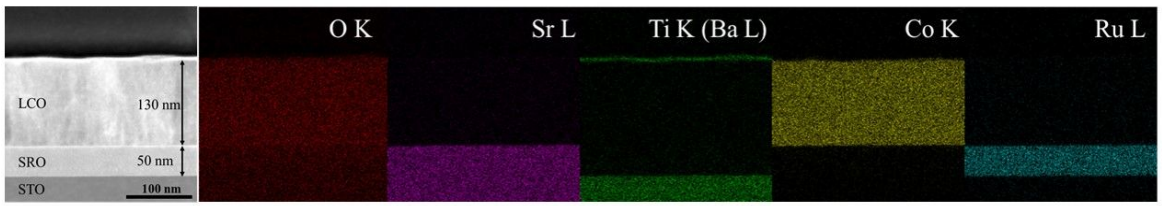

Figure S5. HAADF image and EDX mapping of Planar BTO. HAADF-STEM and EDX measurements were performed on Planar BTO. The thin BTO layer is confirmed by the EDX Ti *K* (Ba *L*) spectra on the top of LCO. The interfaces are clearly separated.

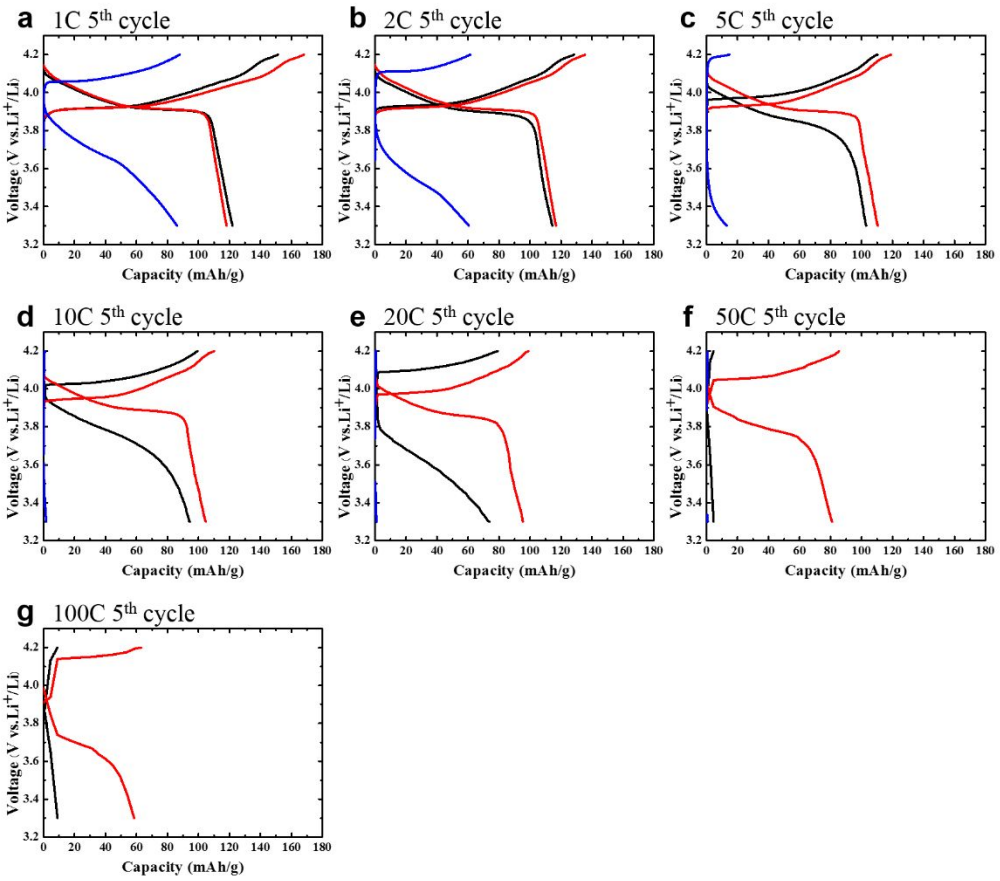

Figure S6. Charge/Discharge curves of Bare(black), Planar BTO(blue) and Dot BTO(red) measured at 5th cycle under 1C, 2C, 5C, 10C, 20C, 50C and 100C.

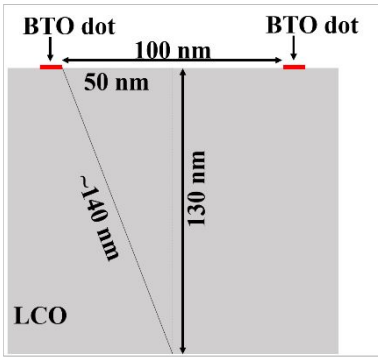

Figure S7. Schematic illustration of cross-sectional Dot BTO. Thickness of LCO layer and distance between BTO dots is 130 nm and 100 nm, respectively. In this case, maximum diffusion length should be ~140 nm.

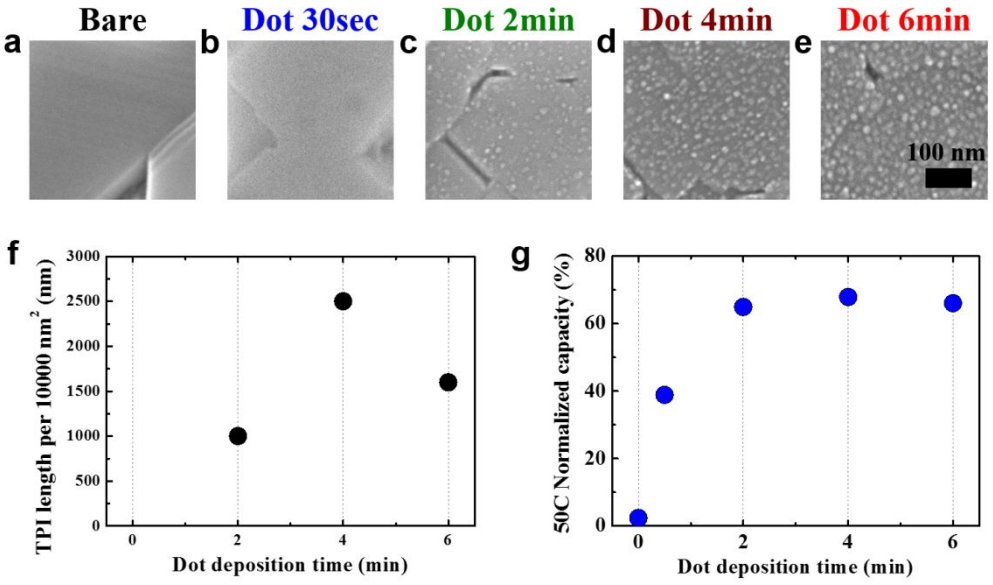

Figure S8. (a)-(e) Plan-view SEM images of Dot BTO with different BTO deposition time. BTO dot density increases with increase of deposition time. (f) TPI length versus BTO dot deposition time. TPI length is calculated at 100 nm x 100 nm area. (g) 50 C normalized discharge capacities versus BTO dot deposition time. Discharge capacity increases with increase of deposition time, then saturated after 2 min deposition.

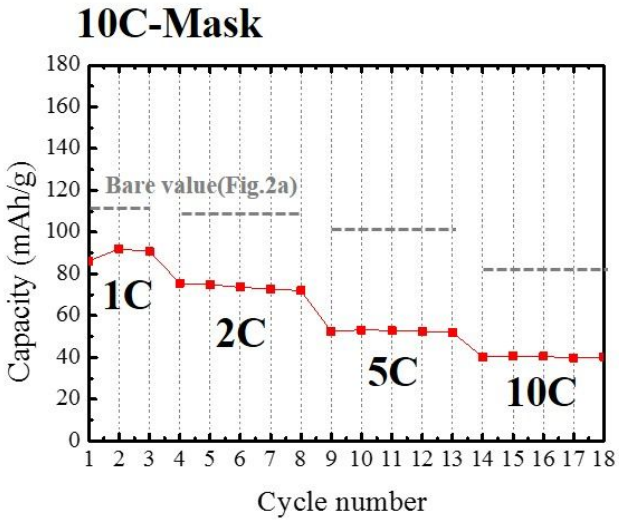

Figure S9. Discharge capacity of 10C-Mask film. Gray dashed lines denote the bare results in Fig. 2a.

Figure S9 shows the discharge capacities of 10C-Mask. Compared with the Bare results, the discharge capacity at 1C of 10C-Mask is 80% of Bare despite of a BTO surface coverage of almost 43%. This result indicates that LCO reacts under the BTO pad through inner diffusion.

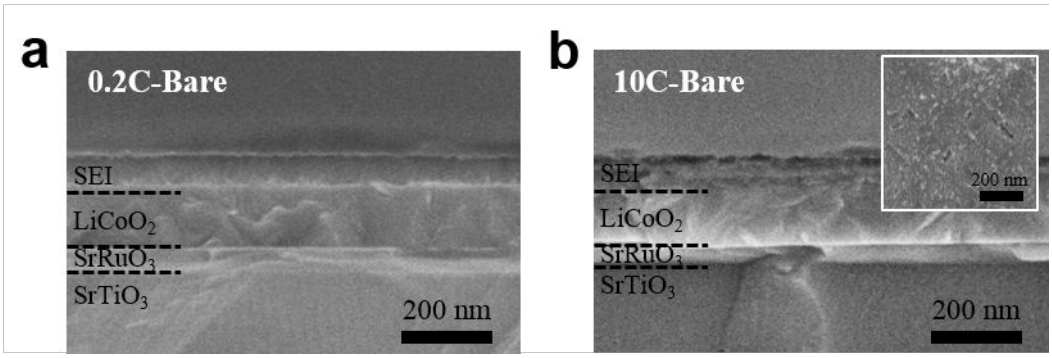

Figure S10. Cross-sectional SEM images of Bare samples after electrochemical cycling under (a) 0.2C and (b) 10C. SEI thickness of each samples are ~100 nm.

References

(1) Watanabe, Y.; Matsumoto, Y.; Kunitomo, H.; Tanamura, M.; Nishimoto, E. *Jpn*. *J*. *Appl*. *Phys*. **1994**, *33*, 5182-5186.

(2) Takeuchi, S.; Tan, H.; Bharathi, K. K.; Stafford, G. R.; Shin, J.; Yasui, S.; Takeuchi, I.; Bendersky, L. A. *ACS Appl*. *Mater*. *Interfaces* **2015**, *7*, 7901-7911.

(3) Li, Z.; Yasui, S.; Takeuchi, S.; Creuziger, A.; Maruyama, S.; Herzing, A. A.; Takeuchi, I.; Bendersky, L. A. *Thin Solid Films* **2016**, *612*, 472-482.

(4) Hirayama, M.; Sonoyama, N.; Abe, T.; Minoura, M.; Ito, M.; Mori, D.; Yamada, A.; Kanno, R.; Terashima, T.; Takano, M.; Tamura, K.; Mizuki, J. *J*. *Power Sources* **2007**, *168*, 493-500.

(5) Ohnishi, T.; Takada, K. *Appl*. *Phys*. *Exp*. **2012**, *5*, 055502.

(6) Ohnishi, T.; Hang, B. T.; Xu, X.; Osada, M.; Takada, K. *J*. *Mater*. *Res*. **2010**, *25*, 1886-1889.